MOMENTA OF INERTIA ALONG THE FISSION PATH FOR Th, U, Pu, Cm, Cf AND Fm NUCLEI

I. AMI[1,2], M. FELLAH[2], N. H. ALLAL[2]

[1]Department of Physics, Faculty of Sciences,
University Mhamed Bougara of Boumerdes,UMBB.
Campus Sud-35000, Boumerdes, Algeria.
E-mail: iami@usthb.dz
[2]Theoretical Physics Laboratory, Faculty of Physics, USTHB.
BP32, El-Alia, 16111 Bab-Ezzouar, Algiers, Algeria.

Received May 21, 2015

Perpendicular, parallel and effective moments of inertia are calculated for deformed doubly even actinide nuclei ranging from $Thorium$ up to $Fermium$ $(226 \leq A \leq 256)$ within the Belyaev cranking-model and by using the single-particle energies and eigenstates of a deformed Woods-Saxon mean field. Calculations had been performed systematically for the ground state, for the second and third minima as well as for the first, second and third saddles points associated with fission isomers. The evolutions of the different momenta of inertia and their dependence on excitation energies as well as on deformations is shown. Comparisons with experimental values, when available, is made.

Keywords: deformed even–even actinide nuclei; effective moment of inertia, excitation energy, deformations.

1. INTRODUCTION

Recently, renewed interest arised for theoretical calculations and predictions for fission isomers properties. This has been, years ago, motivated mainly by the discoveries of the fission isomers and the related resonant structure of the fission cross sections. Theoretical investigations of momenta of inertia on rare-earth and actinides nuclei were able to reproduce the experimental momenta of inertia for equilibrium deformations of nuclei [1, 2]. This had been done by using the cranking formula with pairing correlations, combined with various models such as the liquid drop model or the microscopic-macroscopic model [3] based on the Nilsson [4] or Woods-Saxon [2, 5, 6] shell models, etc. It is well known that the ground state momenta of inertia are reproduced within the limits of $10-25\%$.

Besides, it is well established that the moment of inertia is very sensitive to the pairing correlations. This dependence has been intensively investigated either at zero temperature [2] or at finite temperature [7, 8], and also by including neutron-proton pairing correlations effect at zero [9–12] and at finite temperature [13]. Recently, excitation energy dependence of the moment of inertia for the ^{93}Mo, ^{194}Ir and ^{196}Au nuclei had been performed as a function of the nuclear deformation [5]. These nuclei were recently used in evaluations of induced neutron cross sections and revealed a strong dependence on momentum of inertia parameters. Furthermore, the moment of inertia had been calculated for the ^{240}Pu alpha decay process within the cranking model and using Woods-Saxon two center shell model [6].

Theoretical study of the effective moment of inertia $\Im_{eff}$ represents one of the direct ways to investigate the shape of the nucleus at the barrier [14]. The angular distributions of fission fragments are related to the conservation of angular momentum, and therefore to the moment of inertia in the region comprised between the top of the external barrier to the scission. In the last decades, development in experimental nuclear physics made possible the study of nuclei formed in heavy-ion reactions [15]. It is known that the experimental value of the effective moment of inertia can be obtained from an analysis of the anisotropy of the angular distribution of fission fragments. These fission fragment angular distributions at low spin values and moderate excitation energies are well represented by the means of statistical theory [16, 17]. In this context, the temperature dependence of the moment of inertia can be extracted from data concerning the angular distribution of measured fission fragments anisotropies and the theory can be tested.

The purpose of the present study is to make systematic calculations of the effective moment of inertia at the saddle point as function of mass number and excitation energy. This will be done for the isotopes of some deformed even-even actinides nuclei, *i.e.* $^{226-236}$Th, $^{230-240}$U, $^{236-244}$Pu, $^{240-250}$Cm, $^{248-254}$Cf and $^{252-256}$Fm. Furthermore, systematic calculations of perpendicular and parallel momenta of inertia for the same isotopes nuclei as function of excitation energy for the ground state, the second and third minimum as well as for the first, second and third saddles points are performed.

2. EFFECTIVE MOMENT OF INERTIA

The anisotropy in fission fragment angular distributions is due to a non-uniformity in the distribution of the projections of the total angular momentum along the direction of fission [18]. The anisotropy is generally weak, and in most cases the angular distribution is simply described by the means of the parameter K_0^2. In the statical model, the latter is defined as the mean square value of the projection of angular momentum on the nuclear symmetry axis [4, 19] and is proportional to the product of the effective moment of inertia $\Im_{eff}$ and the temperature T at the saddle point [4, 16, 18]:

$$K_0^2 = \frac{\Im_{eff} T}{\hbar^2} \tag{1}$$

with:

$$\Im_{eff} = \left(\frac{1}{\Im_{\parallel}} - \frac{1}{\Im_{\perp}}\right)^{-1} \tag{2}$$

The temperature dependent momenta of inertia $\Im_{\perp}$ and $\Im_{\parallel}$ are those of a deformed nucleus for a rotation around an axis perpendicular and parallel to symmetry axis respectively.

In the framework of the Inglis cranking model and by taking into account pairing correlations at finite temperature with the Finite Temperature BCS (FTBCS) method, the Belyaev formulas for the perpendicular and parallel momenta of inertia $\Im_{\perp(\parallel)}$ are respectively [1, 20]:

$$\Im_{\perp} = \hbar^2 \sum_{\nu\mu} |\langle\nu|J_x|\mu\rangle|^2 \left\{ \frac{[u_\nu v_\mu - u_\mu v_\nu]^2}{E_\nu + E_\mu} \left(\tanh\frac{\beta E_\nu}{2} + \tanh\frac{\beta E_\mu}{2}\right) \right. \tag{3}$$
$$\left. \frac{[u_\nu u_\mu + v_\nu v_\mu]^2}{E_\nu - E_\mu} \left(\tanh\frac{\beta E_\nu}{2} - \tanh\frac{\beta E_\mu}{2}\right) \right\}$$

and

$$\Im_{\parallel} = \beta\hbar^2 \sum_{\nu} |\langle\nu|J_z|\nu\rangle|^2 \frac{1}{2\cosh^2\left(\dfrac{\beta E_\nu}{2}\right)} \tag{4}$$

where β is the inverse of the temperature T of the system and $J_{x(z)}$ is the single-particle angular momentum operator corresponding to the perpendicular (axial) rotation respectively. E_ν are the quasiparticles energies given by:

$$E_\nu(T) = \sqrt{(\varepsilon_\nu - \lambda - Gv_\nu^2)^2 + \Delta^2(T)} \tag{5}$$

where ε_ν is the single-particle energy in a state $|\nu\rangle$ supposed to be temperature independent [21] and G is a constant pairing force strength. The chemical potential λ and the energy-gap parameter Δ as well as the FTBCS parameters u_ν, v_ν are obtained by resolving the finite-temperature BCS gap equations for a system of an even number of particles n (neutrons or protons):

$$\left\{ \begin{array}{l} \dfrac{1}{G} = \sum\limits_{\nu>0} \dfrac{1}{2E_\nu} \tanh\left(\dfrac{\beta E_\nu}{2}\right) \\ n = \sum\limits_{\nu>0} \left[1 - \dfrac{\varepsilon_\nu - \lambda - Gv_\nu^2}{E_\nu} \tanh(\dfrac{\beta E_\nu}{2})\right] \end{array} \right. \tag{6}$$

The solution of (6) determines the pairing gap Δ and chemical potential λ as a function of T. In the present study, neutron-proton interactions are neglected, so the total $\Im_{\perp(\parallel)}$ for a specific nuclei is the sum between the contribution of protons and neutrons calculated separately.

3. RESULTS AND DISCUSSION

In this work,we considered, doubly even actinides isotopes ranging from $Thorium$ to $Fermium$. The energies and single-particle states are obtained with the Woods-Saxon mean field. The nuclear deformation is described by using the well known Brack parametrization [1, 20, 22, 23]. To characterize the extrema of the potential barrier along the fission path, deformation parameters obtained from fully microscopic calculations are used [24, 25]. If no theoretical deformations are provided, we rely on interpolations and extrapolations procedures.

The pairing strength G is determined from the zero-temperature BCS equations (6) to reproduce the values of the pairing gap parameters $\Delta_p = \dfrac{12}{\sqrt{A}}$ and $\Delta_n = \dfrac{11}{\sqrt{A}}$ (MeV) (A being the mass number), for protons and neutrons respectively [26]. The pairing strengths G are assumed constant, no matter deformation [27, 28].

First of all, systematic calculations of the perpendicular $\Im_\perp$ and parallel momenta of inertia $\Im_\parallel$ were performed for deformed even-even actinides nuclei. The results had been listed in Table 1 for several values of the excitation energy $E^* = 0,\ 5$ and 10 MeV for the ground state deformations. Experimental values of the ground state perpendicular momenta of inertia [1] are also reported in the same table. As it seems, the agreement with the calculated $\Im_\perp$ momenta of inertia and the experimental values is fairly good confirming the fact that the used deformation parameters are consistent. Indeed, the mean relative discrepancy, defined as $|\Im_{\perp \exp} - \Im_\perp|/\Im_{\perp \exp}$ is on average about 8.20%.

Furthermore, calculations of $\Im_\perp$ and $\Im_\parallel$ momenta of inertia were performed for the same nuclei for the second and third minimum as well as at the first, second and third saddles points. Theses calculations had been done for the same values of the excitation energy. The corresponding results are presented in Table 2 up to Table 5. Few experimental values of the momenta of inertia are available for the second and third minimum. Comparing the present calculations at zero excitation energy, one can see that for ^{238,240}Pu and ^{236,238}U nuclei, the mean relative discrepancy between the experimental values [29–32] and the calculated ones for the second minimum does not exceed on average 20%.

The experimental values of the moment of inertia [29–32] at the third minimum are available for only a few of the nuclei of the present study. The comparison at zero excitation energy between them and the theoretical ones shows that for ^{230}Th and ^{232}Th nuclei the mean relative discrepancy is about 15.38% and 3% respectively. The best agreement between the experimental and theoretical data is obtained for an excitation energy of $E^* = 0.3$ MeV in the case of ^{232}Th nucleus, close to the top of the outer barrier. It is a direct confirmation of the fact that the nuclear system is practically cold at the saddle point.

We have then studied the variations of $\Im_{\perp}$ as a function of the mass number A $(226 \leq A \leq 244)$ for U, Th and Pu isotopes chosen as an example. These variations had been done for various excitation energies $E^{*} = 0,\ 5$ and 10 MeV and are given in Fig. 1 for the ground state, second and third minimum as well as for the first, second and third saddle point. Thus, the moment of inertia increases rapidly with the deformation and the temperature. At zero excitation energy, the moment of inertia obtained in the second minimum is more than two times larger than that measured one for the ground state. This ratio is also retrieved for $E^{*} = 5$ and 10 MeV.

We have then studied the variations of the effective moment of inertia $\Im_{eff}$ at the third saddle point as a function of the excitation energy E^{*}. Some examples are presented in Fig. 2. One can see from this figure that for a fixed value of deformation and for each nucleus, the effective moment of inertia values increase with the increase of E^{*}. The dependence of $\Im_{eff}$ upon excitation energy is therefore a good test of the persistence of superconducting effects to finite excitation energies [4]. It is worth noticing that M. Sano *et al.* [4] obtained a similar curve for the ^{242}Pu nucleus at the second saddle point where agreement with experimental values is good.

In Fig. 3, the variations of $\Im_{eff}$ at the third saddle point as a function of mass number A for a given excitation energy are presented for $E^{*} = 10$ MeV. This value of the excitation energy is close to the averaged dissipated energy in fission at scission [33]. As displayed in Fig. 3, the effective momenta of inertia variations as a function of mass numbers are not constant. In fact, Th and U isotopes effective momenta of inertia exhibit the same trends with regard to mass numbers A, whereas, Pu, Cf and Fm isotopes have another ones.

In conclusion, a systematic calculations of the perpendicular, parallel and effective moments of inertia of various doubly even actinides nuclei ranging from $Thorium$ to $Fermium$ $(226 \leq A \leq 256)$ for the ground state, second and third minimum as well as for the first, second and third saddle point as a function of excitation energy had been performed. Comparison with experimental values of momenta of inertia, when available, had been made.

Acknowledgements. This work was performed under a Grant of the Department of Physics, Faculty of Sciences, University M'hammed Bougara of Boumerdes UMBB. The authors thank M. Mirea for useful and interesting discussions.

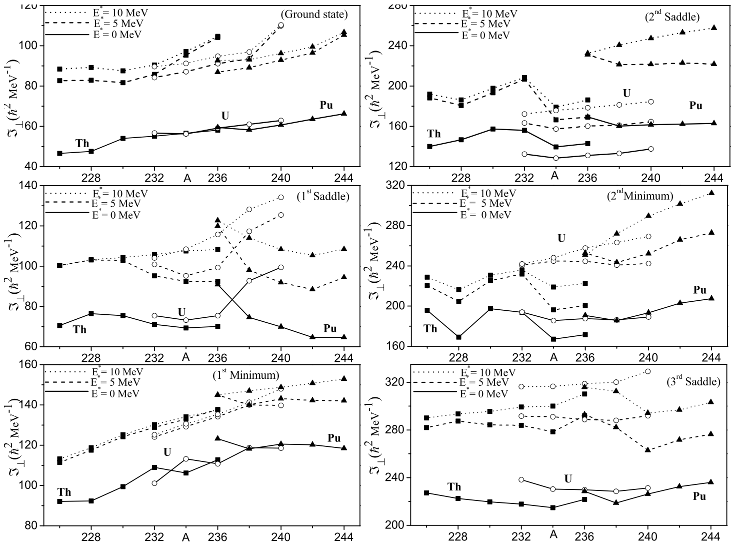

Fig. 1 – Dependence of Th, U and Pu perpendicular momenta of inertia as function of mass number A $(228 \leq A \leq 256)$, for ground state, second and third minimum as well as for the first, second and third saddle points. The values of the excitation energy E^* are 0, 5 and 10 MeV and are marked on the plot.

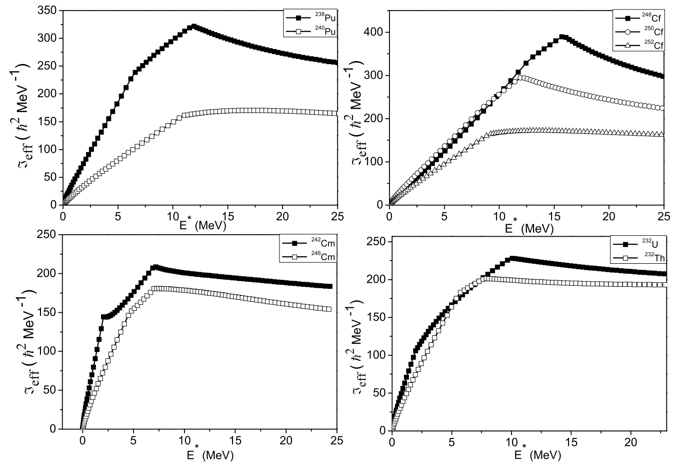

Fig. 2 – The effective moment of inertia $\Im_{eff}$ of the third saddle point as a function of the excitation energy for different nuclei: ^{238,240}Pu, ^{242,246}Cm, ^{248,250,252}Cf, ^{232}U and ^{232}Th chosen as an example.

Table 1

Perpendicular and parallel momenta of inertia calculated for the the ground state (g.s) deformations, in the case of doubly even actinides nuclei at different excitation energies. Experimental values are those of Ref. [1].

Nucleus	$\Im_{\perp}(\hbar^2\mathrm{MeV}^{-1})_{gs}$			$\Im_{\parallel}(\hbar^2\mathrm{MeV}^{-1})_{gs}$		$\Im_{\perp\,\exp}(\hbar^2\mathrm{MeV}^{-1})_{gs}$
	E^* (MeV)			E^* (MeV)		
	0	5	10	5	10	
^{226}Th	46.54	82.62	88.425	92.82	94.06	41
^{228}Th	47.58	82.85	89.20	79.84	87.84	52
^{230}Th	53.96	81.69	87.51	92.23	95.91	56
^{232}Th	55.10	85.77	90.50	80.41	88.47	60
^{234}Th	56.54	95.29	97.14	80.46	85.40	63
^{236}Th	58.09	104.01	104.71	89.75	90.70	
^{232}U	56.64	84.22	89.72	98.73	99.88	63
^{234}U	56.26	87.06	91.27	72.70	83.55	69
^{236}U	59.07	91.12	94.73	80.58	88.24	66
^{238}U	61.03	93.60	96.88	78.41	85.81	67
^{240}U	62.86	109.90	110.31	87.59	92.78	———
^{236}Pu	59.48	86.84	92.71	95.08	98.67	67
^{238}Pu	58.27	89.07	93.11	61.04	75.42	68
^{240}Pu	60.70	92.89	96.28	69.57	81.12	70
^{242}Pu	63.52	96.41	99.47	71.08	81.43	67
^{244}Pu	66.27	105.28	106.71	79.20	87.22	67
^{240}Cm	62.52	91.34	96.49	96.52	98.65	———
^{242}Cm	61.93	90.62	95.14	71.59	83.39	71
^{244}Cm	63.59	103.12	104.70	79.12	87.55	70
^{246}Cm	66.12	105.50	107.01	79.73	88.24	70
^{248}Cm	68.08	108.43	109.80	81.30	90.29	69
^{250}Cm	70.70	113.74	114.57	90.25	99.74	———
^{248}Cf	67.96	106.86	108.36	83.98	93.83	71
^{250}Cf	69.37	106.70	108.95	78.83	90.77	68
^{252}Cf	70.62	112.65	113.71	88.51	98.35	68
^{254}Cf	70.34	113.02	115.65	96.52	103.60	———
^{252}Fm	71.57	108.24	110.15	83.28	95.61	———
^{254}Fm	71.42	112.05	113.24	90.68	98.76	68
^{256}Fm	76.86	113.00	114.82	147.37	135.16	———

Table 2

Perpendicular momenta of inertia calculated at the first saddle, second minimum and second saddle.

Nucleus	$\Im_\perp(\hbar^2\text{MeV}^{-1})_{1^{st}\text{saddle}}$			$\Im_\perp(\hbar^2\text{MeV}^{-1})_{2^{nd}\text{min}}$			$\Im_\perp(\hbar^2\text{MeV}^{-1})_{2^{nd}\text{saddle}}$		
	E^* (MeV)			E^* (MeV)			E^* (MeV)		
	0	5	10	0	5	10	0	5	10
^{226}Th	70.54	100.29	100.29	92.16	111.50	113.17	140.06	188.23	191.91
^{228}Th	76.46	103.15	103.22	92.36	117.56	118.74	146.71	180.56	186.22
^{230}Th	75.48	102.93	104.36	99.48	124.25	125.22	157.24	193.44	197.76
^{232}Th	71.20	95.19	105.77	109.04	128.93	130.21	155.92	206.87	208.52
^{234}Th	69.31	92.46	107.50	106.19	133.01	134.17	139.52	166.43	179.19
^{236}Th	70.09	92.47	108.30	112.76	137.81	137.52	142.82	169.04	186.19
^{232}U	75.46	100.91	104.14	101.11	124.16	125.21	132.49	163.38	172.25
^{234}U	73.17	95.18	108.40	113.21	129.19	130.65	128.40	157.37	175.80
^{236}U	75.48	99.30	115.76	110.82	134.28	135.39	131.17	160.29	178.45
^{238}U	92.74	117.35	128.17	118.78	140.03	141.28	133.13	161.14	181.31
^{240}U	99.46	125.47	134.20	118.60	139.83	147.98	137.46	164.60	184.35
^{236}Pu	90.86	119.85	122.64	123.23	144.91	145.04	169.25	231.22	232.39
^{238}Pu	74.56	97.97	113.97	118.25	140.02	146.96	160.16	221.34	240.67
^{240}Pu	69.89	91.87	108.28	120.54	143.10	148.77	161.50	221.54	247.30
^{242}Pu	64.70	88.43	105.34	120.17	142.25	150.73	162.20	222.97	253.10
^{244}Pu	64.71	94.42	108.47	118.47	142.06	152.87	162.97	221.87	257.54
^{240}Cm	63.89	91.46	99.95	135.19	156.52	159.61	128.08	158.89	161.77
^{242}Cm	63.64	87.05	101.74	130.58	151.43	161.71	138.33	165.43	175.28
^{244}Cm	62.57	83.85	101.63	126.41	147.80	162.10	145.28	172.23	189.61
^{246}Cm	68.34	90.45	108.16	123.23	145.14	159.72	162.01	190.55	208.54
^{248}Cm	81.26	103.77	122.79	125.90	148.54	164.86	183.95	214.45	231.15
^{250}Cm	87.38	109.85	128.12	128.47	150.80	167.45	206.15	242.20	254.80
^{248}Cf	92.40	117.66	134.11	122.49	144.02	159.75	129.38	154.31	169.84
^{250}Cf	97.36	121.36	137.10	125.59	148.43	162.72	133.00	159.36	171.97
^{252}Cf	101.08	124.34	140.12	127.53	150.54	165.54	135.11	161.37	174.08
^{254}Cf	109.61	131.66	144.61	130.53	153.71	167.76	130.53	153.71	167.76
^{252}Fm	33.69	77.28	104.47	65.71	117.65	137.32	65.03	123.06	154.22
^{254}Fm	67.01	93.90	106.93	108.52	146.50	156.65	95.46	123.14	143.91
^{256}Fm	129.42	158.83	164.71	171.84	194.74	204.00	142.43	168.30	180.55

Table 3

Same as Table 2 at the third minimum and the third saddle point.

Nucleus	$\Im_{\perp}(\hbar^2\mathrm{MeV}^{-1})_{3^{rd}\mathrm{min}}$			$\Im_{\perp}(\hbar^2\mathrm{MeV}^{-1})_{3^{rd}\mathrm{saddle}}$		
	E^* (MeV)			E^* (MeV)		
	0	5	10	0	5	10
^{226}Th	195.90	220.26	228.79	227.25	282.00	290.13
^{228}Th	169.15	204.67	216.27	222.47	287.46	293.44
^{230}Th	197.41	225.30	230.86	219.68	284.28	295.60
^{232}Th	193.77	231.82	235.95	217.79	283.91	299.39
^{234}Th	167.13	196.35	219.07	214.77	278.40	300.06
^{236}Th	171.52	200.60	222.50	221.81	292.03	310.29
^{232}U	193.98	240.64	241.94	238.22	291.61	316.33
^{234}U	185.63	244.68	248.21	230.46	291.10	316.64
^{236}U	187.53	244.53	257.73	229.84	288.85	318.80
^{238}U	186.34	240.67	263.27	228.60	288.14	320.22
^{240}U	189.20	242.32	269.21	231.37	291.976	329.27
^{236}Pu	190.79	252.82	250.87	228.56	293.03	315.88
^{238}Pu	185.51	243.55	272.03	218.80	282.16	312.49
^{240}Pu	193.42	252.18	289.42	226.33	262.94	294.22
^{242}Pu	203.03	265.92	301.48	232.57	271.74	296.81
^{244}Pu	207.43	272.74	312.14	236.06	276.43	303.31
^{240}Cm	149.86	179.44	182.65	154.28	189.94	190.48
^{242}Cm	155.81	183.87	199.19	152.42	186.60	194.48
^{244}Cm	169.89	199.18	218.35	192.74	233.16	254.38
^{246}Cm	189.81	223.45	243.48	236.60	283.35	291.40
^{248}Cm	218.87	264.08	277.74	280.05	333.01	329.26
^{250}Cm	252.08	303.63	304.19	328.37	392.80	384.20
^{248}Cf	153.47	178.50	194.73	138.15	174.65	200.29
^{250}Cf	187.88	226.01	238.56	186.65	224.51	252.62
^{252}Cf	209.49	249.92	259.91	247.82	296.08	324.24
^{254}Cf	243.69	293.62	294.34	327.13	392.96	389.68
^{252}Fm	68.73	89.88	108.28	103.17	133.54	147.19
^{254}Fm	90.17	113.60	131.70	95.46	123.14	143.91
^{256}Fm	106.03	125.69	140.63	121.74	128.61	150.83

Table 4

Same as Table 2, for the parallel momenta of inertia.

Nucleus	$\Im_{\parallel}(\hbar^2 MeV^{-1})_{1^{st}\text{saddle}}$		$\Im_{\parallel}(\hbar^2 MeV^{-1})_{2^{nd}\text{min}}$		$\Im_{\parallel}(\hbar^2 MeV^{-1})_{2^{nd}\text{saddle}}$	
	E^* (MeV)		E^* (MeV)		E^* (MeV)	
	5	10	5	10	5	10
^{226}Th	108.04	113.93	78.97	76.79	67.68	74.52
^{228}Th	87.81	101.07	86.28	79.98	41.75	54.92
^{230}Th	84.52	100.36	79.90	82.22	40.72	55.10
^{232}Th	75.55	102.00	77.59	84.05	49.91	63.41
^{234}Th	73.69	105.07	87.58	87.00	71.18	91.17
^{236}Th	72.95	104.27	92.16	89.45	77.54	102.08
^{232}U	83.80	104.45	68.93	76.65	72.72	96.74
^{234}U	70.60	99.63	70.56	78.36	71.21	102.79
^{236}U	74.30	105.21	74.83	82.96	76.93	107.25
^{238}U	85.00	104.37	81.31	89.89	76.64	110.00
^{240}U	105.85	104.43	92.52	100.94	75.00	108.15
^{236}Pu	82.80	91.06	108.60	99.36	79.74	83.64
^{238}Pu	64.80	95.37	89.64	102.46	73.17	93.46
^{240}Pu	60.75	95.86	94.38	104.52	78.35	104.74
^{242}Pu	84.59	122.71	91.64	107.15	81.52	112.81
^{244}Pu	99.49	121.02	93.12	110.86	79.93	116.93
^{240}Cm	109.95	114.92	106.25	102.74	123.54	109.43
^{242}Cm	101.70	129.69	97.96	112.01	102.95	111.15
^{244}Cm	76.43	116.61	90.89	117.18	92.10	109.39
^{246}Cm	66.41	104.89	90.99	117.01	88.68	104.67
^{248}Cm	69.95	111.69	92.92	123.44	94.10	107.52
^{250}Cm	74.76	115.75	91.74	121.63	107.26	114.73
^{248}Cf	75.40	108.48	90.42	118.83	100.64	124.92
^{250}Cf	76.43	108.33	94.34	119.07	109.05	124.82
^{252}Cf	71.75	105.09	91.69	117.59	107.68	122.62
^{254}Cf	69.43	99.70	92.34	115.67	92.34	115.67
^{252}Fm	110.82	170.53	89.92	122.07	91.45	135.21
^{254}Fm	81.94	115.79	61.16	77.20	58.10	91.00
^{256}Fm	88.62	93.803	86.23	104.76	97.54	115.17

Table 5

Same as Table 3, for the parallel momenta of inertia.

Nucleus	$\Im_{\parallel}(\hbar^2\text{MeV}^{-1})_{3^{rd}min}$		$\Im_{\parallel}(\hbar^2\text{MeV}^{-1})_{3^{rd}\ Saddle}$	
	E^* (MeV)		E^* (MeV)	
	5	10	5	10
^{226}Th	39.22	56.81	96.44	99.32
^{228}Th	71.64	84.92	111.69	108.68
^{230}Th	43.82	57.83	111.11	115.16
^{232}Th	50.55	61.83	103.88	119.63
^{234}Th	56.69	85.76	93.74	123.15
^{236}Th	59.24	88.02	102.83	128.13
^{232}U	76.91	78.44	106.01	132.55
^{234}U	91.48	91.19	102.49	134.22
^{236}U	93.60	105.06	103.27	139.62
^{238}U	92.66	118.04	109.31	146.56
^{240}U	95.22	128.07	114.69	162.92
^{236}Pu	107.59	98.41	121.16	148.69
^{238}Pu	99.04	131.43	110.62	151.49
^{240}Pu	99.46	146.91	60.74	107.56
^{242}Pu	99.49	144.69	68.86	106.49
^{244}Pu	103.92	152.17	76.39	118.17
^{240}Cm	101.12	99.43	92.36	93.64
^{242}Cm	92.11	102.78	90.84	98.82
^{244}Cm	88.93	104.05	100.33	116.23
^{246}Cm	99.68	115.32	100.3907	110.79
^{248}Cm	124.85	128.11	141.0274	123.89
^{250}Cm	142.48	129.54	152.1115	119.38
^{248}Cf	74.91	101.73	72.94807	111.40
^{250}Cf	86.41	104.52	84.91559	127.04
^{252}Cf	107.68	114.11	71.28411	110.24
^{254}Cf	140.78	129.30	106.6443	98.43
^{252}Fm	68.94	109.35	62.9415	88.29
^{254}Fm	67.37	105.65	58.10	91.00
^{256}Fm	77.51	109.62	10.90	60.55

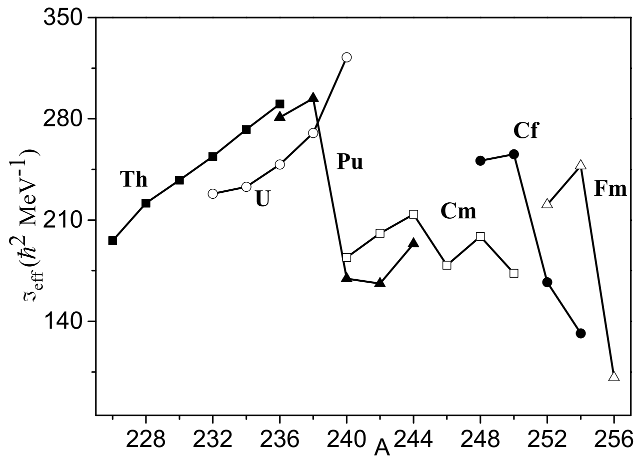

Fig. 3 – Variation of the effective moment of inertia $\Im_{eff}$ of the third saddle point as a function of mass number A $(228 \leq A \leq 256)$ for deformed doubly even actinides nuclei evaluated at excitation energy $E^* = 10$ MeV.

REFERENCES

1. M. Brack, T. Ledergerber, H.C. Pauli, A.S. Jensen, Nucl. Phys. **A 234**, 185–215 (1974).
2. N.H. Allal and M. Fellah, Phys. Rev. **C 43**, 2648–2657 (1991).
3. A. Iwamoto, S. Y. Amaji, S. Suekane and K. Harada, Prog. Theor. Phys. **55**, 115-130 (1976).
4. M. Sano M. Wakai, Prog. Theor. Phys. **48**, 160-181 (1972).
5. I. Ami, M. Fellah, N.H. Allal and M.R. Oudih, Rom. J. Phys. **59**, 504–513 (2014).
6. M. Mirea, Rom. J. Phys. **60**, 156-160 (2015).
7. N.H. Allal, M. Fellah, N. Benhamouda, and M.R. Oudih, Phys. Rev. **C 77**, 054310–8 (2008).
8. Y. Alhassid, G. F. Bertsch, L. Fang and S. Liu, Phys. Rev. **C 72**, 064326-11 (2005).
9. D. Mokhtari, I. Ami, M. Fellah and N. H. Allal, Int. J. Mod. Phys. **E 17**, 655-667 (2008).
10. M. Gerceklioğlu and A. E. Calik, Acta. Phys. Slo. **55**, 197-209 (2005).
11. E. Meftunoğlu *et al.*, J. Phy. G : Nucl. Part. Phys. **24**, 107-115 (1998).
12. A. E. Calik, C. Deniz and M. Gerceklioglu, Pramana. J. Phys. **73**, 847-857.
13. I. Ami, M. Fellah, N. H. Allal, N. Benhamouda, M. Belabbas and M. R. Oudih, Int. J. Mod. Phys. **E 20**, 1947-1959 (2011).
14. R. W. Hasse, Ann. Phys., **68**, 377-461 (1971).
15. E. G. Ryabov and G. D. Adeev, Phys. Atom. Nucl. **68,** 1525-1539 (2005).
16. J. R. Huizenga, A. N. Behkami and L. G. Moretto, Phys. Pev. **177**, 1826-1830 (1969).
17. I. S. Grant, Rep. Prog. Phys. **39**, 955-1015 (1976).
18. S. Bjørnholm and V. M. Strutinsky, Nucl. Phys. **A136**, 1-24 (1969).
19. R. Razavi and V. Dehghani, Int. J. Mod. Phys.**E 23**, 1450015–7 (2014).
20. Brack, J. Damgaard, A.S. Jensen, H.C. Pauli, V.M. Strutinsky and C.Y.Wong, Rev. Mod. Phys. **44**, 320–405 (1972).
21. M. Brack and P. Quentin, Nucl. Phys. **A 361**, 35–82 (1981).
22. R. W. Hasse and W. D. Myers, Geometrical Relationship of Macroscopic Nuclear Physics (Springer-Verlag, Heidelberg, 1988).
23. H.C. Pauli, Phys. Rep. **7**, 35-100 (1973).
24. S. Goriely, M. Samyn, J.M. Pearson, Phys. Rev. **C 75**, 064312-7 (2007).
25. S. Goriely, Private communication.
26. H. J. Krappe, K. Pomorski, Theory of Nuclear Fission, Lecture Notes in Physics, Vol. 838, (Springer-Verlag, Heidelberg, 1988).
27. A. Sobiczewski, S. Bjørnholm and K. Pomorski, Nucl. Phys. **A 202**, 274–288 (1973).
28. K. Pomorski, Acta. Phys. Pol. **B 9**, 61-69 (1978).
29. S. Bjørnholm, J. E. Lynn, Rev. Mod. Phys. **52**, 725-931 (1980).
30. I. Hamamoto, Phys. Lett. **56B**, 431-435 (1975).
31. I. Blons, C. Mazur, D. Paya, M. Ribrag and H. Weigmann, Nucl. Phys. **A 414**, 1-41 (1984).
32. H. Backe, L. Richter, D. Habs, V. Metag, J. Pedersen, P. Singer, and H. J. Specht, Phys. Rev. Lett. **42**, 490-493 (1979).
33. N.S. Shakib, M.F. Rahimi and M.M. Firoozabadi, Rom. Rep. Phys. **65**, 401-410 (2013).